Development of a numerical model to study the dispersion of wastes coming from a marine fish farm in the Ligurian Sea (Western Mediterranean)

A. M. Doglioli [a], M. G. Magaldi [a], L. Vezzulli [b], S. Tucci [b]

[a] *INFM, National Institute for the Physics of Matter - DIFI, Department of Physics, University of Genova, Via Dodecaneso 33, I-16146 Genova, Italy*

[b] *DIPTERIS, Department for the Study of Territory and its Resources, University of Genova, corso Europa 26, I-16132 Genova, Italy*

Abstract

In order to simulate the dispersion of pollutants released from a marine fish farm in the Ligurian Sea (Western Mediterranean), the Lagrangian particle model LAMP3D has been nested into the numerical hydrodynamical model POM. Estimates of the regional dispersion patterns of nitrogen, phosphorus and organic carbon were calculated using a three dimensional mesoscale grid and compared to in situ experimental data. In the numerical simulations the dispersion of different aquaculture wastes (dissolved nutrients, faecal matter and feed wastes) was evaluated by changing the rates of particles settling and their condition of release (continuous or periodical). Result of the simulations clearly showed that dissolved particles tend to spread rapidly and undergo rapid dilution depending on dominant wind and surface currents direction. In contrast settling particles remain mainly confined in the fish farm area and readily sink. Predicted concentrations of wastes were low in both the water column and sediment compartments and never exceed the threshold of environmental crises.

Key words: Modelling; Aquaculture impact; Mediterranean; Husbandry; Net-pen; Organic matter;

1 Introduction

Fish farming is rapidly developing in the Mediterranean and the potential for detrimental effects on the marine environment is becoming an issue of public interest. Release of organic wastes might determine changes in the community

structure and biodiversity of the benthic assemblages (Tsutsumi et al., 1991; Wu et al., 1994; Vezzulli et al., 2002, In press). Faeces and medicated feed are also of concern (Wu, 1995; Sørensen et al., 1998; Chelossi et al., 2003). For this reason before a new farm is established, or an increase in production of an existing farm permitted, the potential impact of the farm on its surrounding environment should be assessed.

Mathematical models have been developed for policies and procedures to minimize net-pen aquaculture impacts (Henderson et al., 2001). Gowen et al. (1989) were pioneers in developing such models. They used analytical models describing dispersion in a constant flow in time and space. Successively, Gillibrand and Turrell (1997) implemented models with many simplifying assumptions about hydrography. Recently, Cromey et al. (2002a) developed the particle tracking model DEPOMOD, including hydrographic data for modeling resuspension and changes in the benthic faunal community. Hydrodynamic models of settling, resuspension and decay of net-pen wastes coupled with transport models were also used for assessing the environmental impacts of marine aquaculture (Panchang et al., 1997; Dudley et al., 2000). However, most of these models use only two-dimensional equations and the shear in the water column, where velocity changes over depth, is still not modeled. In addition these models do not take into account the different kinds of pollutants (e.g. nitrogen, phosphorus,organic carbon) with their typical deposition rates.

In this study, we developed a 3D numerical model by coupling a three dimensional Lagrangian model, LAMP3D (Lagrangian Assessment for Marine Pollution 3 Dimensional model), into the hydrodynamical model POM (Princeton Ocean Model) in order to describe both the 3D hydrodynamic flows and the 3D dispersion phenomena of pollutants coming from a marine fish cage in the Mediterranean Sea. LAMP3D is able to provide vertical profiles by using POM vertically averaged flow field to compute a theoretical vertical profile of the finite bottom Ekman spiral. Furthermore, LAMP3D can be used for simulations of dispersion with different pollutants (dissolved nutrients, faecal pellets and uneaten feed) and/or with different conditions of release (continuous or periodical).

2 Methods

2.1 Study area

The simulation was carried out for a coastal fish farm located east of Lavagna in the Ligurian Sea (Fig. 1). The sea cages are located at about 1.5 km distance from the coast and cover an area of $2 \cdot 10^5$ m^2. The depth ranges

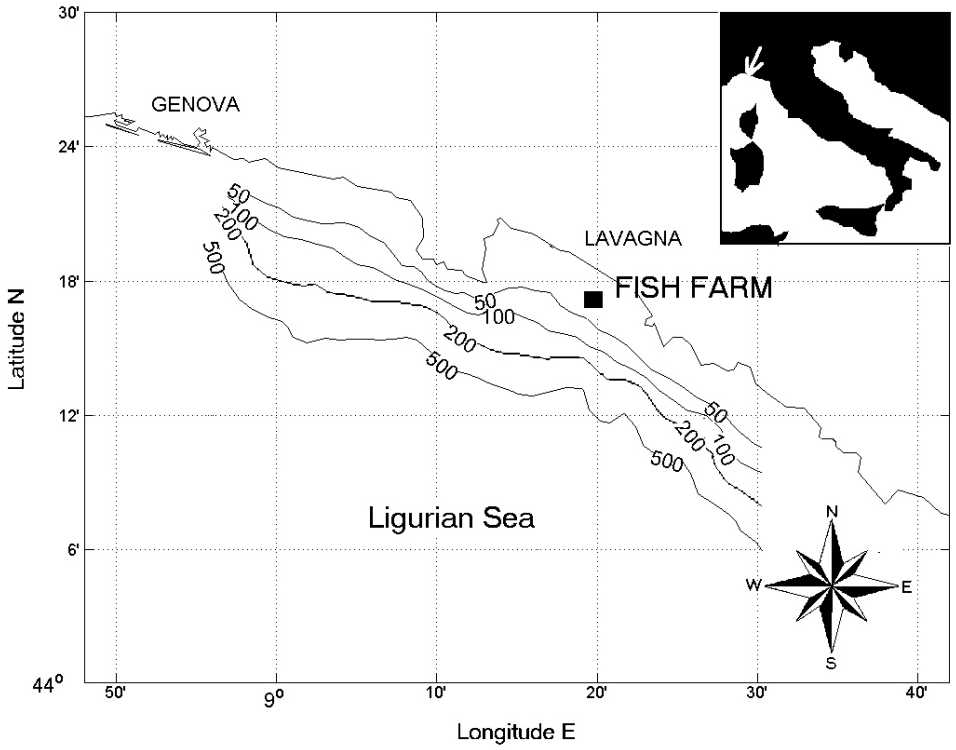

Fig. 1. Study area and fish farm location.

between 38 m and 41 m.

The farm is composed of 8 fish cages (2000 m^3 each) with a reared biomass of 20 kg/m^3 for a production of about 200 ton/year. Reared fish are mostly Gilthead Sea Bream (*Sparus aurata*) and Sea Bass (*Dicentrarchus labrax*) to a lesser extent.

2.2 The transport model LAMP3D

LAMP3D is a single-particle lagrangian model (Doglioli, 2000): at each time step Δt a particle moves from its position $\boldsymbol{r} = (x, y, z)$ with a velocity $\mathbf{v}(\boldsymbol{r}(t), t)$ causing a displacement, which determines the new position of a particle in a time interval $\Delta t = t_2 - t_1$

$$\mathbf{r}(t_1 + \Delta t) = \mathbf{r}(t_1) + \int_{t_1}^{t_1+\Delta t} \mathbf{v}\Big(\mathbf{r}(t), t\Big)\, dt\,.$$

The total velocity $\mathbf{v}(\boldsymbol{r}(t),t)$ is formed by $\mathbf{U}(\boldsymbol{r}(t),t)$ and $\mathbf{v}'$ (Zannetti, 1990),

$$\mathbf{v} = \mathbf{U} + \mathbf{v}' \,,$$

where $\mathbf{U}$ is the calculated flow field (representing the transport process due to the mean flow field), while $\mathbf{v}'$ is a stochastic fluctuation, which is related to the turbulence and small scale eddies.

In this study, the time and space scales of the dispersion processes allow to use a simple 'random walk model' (Allen, 1982):

$$\mathbf{r}_{\mathrm{n}+1} - \mathbf{r}_{\mathrm{n}} = \mathbf{U}_{\mathrm{n}} \Delta t + \boldsymbol{\varrho}_{\mathrm{n}} \,.$$

To assign a value to $\boldsymbol{\varrho} = (\varrho_{\mathrm{x}}, \varrho_{\mathrm{y}}, \varrho_{\mathrm{z}})$ the LAMP3D algorithm uses the FORTRAN generator of pseudorandom numbers with uniform distribution in the interval $[0,1]$ to obtain a normal probability density function with zero mean and given standard deviation $\boldsymbol{\sigma} = (\sigma_{\mathrm{x}}, \sigma_{\mathrm{y}}, \sigma_{\mathrm{z}})$.

Thus, for a cloud of Q diffusing particles released in the absence of velocity from a single point $P(0,0,0)$ at time $t = 0$, their space distribution at some time later $t = n\Delta t$ is

$$C(\mathbf{r}, n) = \frac{Q}{(2\pi n \boldsymbol{\sigma}^2)^{3/2}} \left(e^{-\frac{\mathbf{r}^2}{2\mathrm{n}\sigma^2}} \right) \,. \tag{1}$$

This is identical to the point source Gaussian solution

$$G(\boldsymbol{r}, t) = \frac{1}{(4\pi \kappa_{\mathrm{q}} t)^{3/2}} \left(e^{-\frac{\mathbf{r}^2}{(4\kappa \mathrm{q} t)}} \right) \tag{2}$$

for the standard diffusion equation for the property q

$$\frac{\partial q}{\partial t} = \kappa_{\mathrm{q}} \, \partial^2 q \,,$$

where κ_{q} is the diffusion coefficient, measured in m^2/s.

The model input parameter $\boldsymbol{\sigma}$ is given by

$$\boldsymbol{\sigma} = \sqrt{2\kappa_{\mathrm{q}} \Delta t}$$

in meters. A comparison between the 'K-theory' κ_{q} coefficient and experimental data given by Bacciola et al. (1993) allows a suitable choice of the value

$\boldsymbol{\sigma} = 3.46$ m.

Our model uses a constant standard deviation value on the horizontal grid $\sigma_{\mathrm{i,j}} = \sigma_{\mathrm{x}} = \sigma_{\mathrm{y}}$ which decreases, as the intensity of turbulent processes, with the depth:

$$\sigma_{\mathrm{i,j}}(z_{\mathrm{n}}) = \sigma_{\mathrm{i,j}}(0)\left(1 + \frac{z_{\mathrm{n}}}{H_{\mathrm{i,j}}}\right),$$

where z_{n} is the vertical coordinate of the particle and $H_{\mathrm{i,j}}$ is the local bathymetry value.

We used 86400 particle in our simulations. This value adequately represents the plume and is accetable in terms of the required computational time. In previous works, Doglioli (2000) and Magaldi (2002) performed several tests comparing the numerical results provided by LAMP3D both with analytical solutions in simplified cases and with the results provided by the Eulerian numerical model MIKE21 (www.dhisoftware.com/mike21/). The particles are released homogeneously from the grid mesh corresponding to the fish farm domain at a depth of 10 m. Specific properties can be assigned to each single particle. In this study (1) conservative, (2) decaying and (3) settling particles have been considered.

(1) conservative particle number is constant for the whole duration of the simulation, except if particles cross the open boundaries or if there is a source in the domain.
(2) An exponential decay which uses the T_{90} parameter (the time required to degrade 90% of the biodegradable matter in a given environment (Vismara, 1992)) is applied to decaying particles:

$$c = c_0 \cdot 10^{-\frac{\mathrm{t}}{\mathrm{T}_{90}}}.$$

(3) A sedimentation velocity $\boldsymbol{w}_{\mathrm{sed}} = (0, 0, w_{\mathrm{sed}})$ is added to deterministic velocity $\mathbf{U}$ of settling particles.

At the end of each suitably chosen time interval the concentration field $C_{\mathrm{i,j,k}}$ is computed by simply counting the number of particles found within each grid cell.

2.3 The POM-LAMP3D coupled model

In order to simulate the 3D dispersion of wastes from the fish farm the LAMP3D transport model was coupled to the Princeton Ocean Model, POM

(Mellor, 1998). The POM FORTRAN77 code is freely distributed (www.aos.-princeton.edu/WWWPUBLIC/htdocs.pom/). POM is a three-dimensional, finite difference, free surface numerical model utilizing the Boussinesq and the hydrostatic approximations and mode split time step. The mode split technique allows the two-dimensional calculation of the free surface elevation and the velocity transport in barotropic approximation separately from the three-dimensional calculation of velocity and thermodynamics (baroclinic mode). For this preliminary study only the 2D scheme (POM2D) was used. A suitable, although approximate, method was then used to build a 3D flow field.

POM2D solves the equation of the free surface elevation and the momentum equations integrated from bottom ($\varsigma = -1$) to surface ($\varsigma = 0$) and provides the horizontal vertically averaged velocity component

$$\overline{U} = \int_{-1}^{0} U \mathrm{d}\varsigma\,, \qquad \overline{V} = \int_{-1}^{0} V \mathrm{d}\varsigma\,.$$

The LAMP3D model calculates the 3D velocity field $\mathbf{U}_{\mathrm{i,j,k}} = (u_{\mathrm{i,j,k}}, v_{\mathrm{i,j,k}}, w_{\mathrm{i,j,k}})$ using mass conservation and theoretical vertical velocity profiles (Doglioli, 2000). In this study we obtain good results whith the vertical profile based on the Ekman spiral model. Even if the Ekman spiral profile details have been very rarely measured, the effects of the transport integral on the water column has been frequently observed both in deep and in coastal waters. In this way, using the mean horizontal velocity vector provided by POM2D ($\mathbf{v}_{\mathrm{i,j}}^{\mathrm{POM2D}}$) the horizontal velocity $\mathbf{v}_{\mathrm{i,j,k}}^{\mathrm{H}} = (u_{\mathrm{i,j,k}}, v_{\mathrm{i,j,k}})$ at a given depth $k\Delta z$ can be calculated by the formula

$$\mathbf{v}_{\mathrm{i,j,k}}^{\mathrm{H}} = \mathbf{v}_{\mathrm{i,j}}^{\mathrm{POM2D}}\, \kappa H_{\mathrm{i,j}}\, \frac{e^{\kappa(\mathrm{H+k})} - e^{-\kappa(\mathrm{H+k})}}{\left(e^{\frac{\kappa \mathrm{H}}{2}} - e^{\frac{-\kappa \mathrm{H}}{2}}\right)^2}\,,$$

where

$$\kappa = (1+\imath)\frac{\pi}{\left(\frac{\delta_{\mathrm{E}}}{\Delta Z}\right)}$$

is a complex ($\imath$ is the imaginary unit) function of Ekman depth $\delta_{\mathrm{E}} = 150$ m.

The code imposes the mass conservation in each grid cell and calculates a 3D field for the vertical component of the velocity:

$$w_{\mathrm{i,j,k}} = w_{\mathrm{i,j,k+1}} + \Delta Z \left(\mathrm{Re}\left\{ \frac{\mathbf{v}_{\mathrm{i+1,j,k}}^{\mathrm{POM2D}} - \mathbf{v}_{\mathrm{i-1,j,k}}^{\mathrm{POM2D}}}{2\Delta X} \right\} + \mathrm{Im}\left\{ \frac{\mathbf{v}_{\mathrm{i,j+1,k}}^{\mathrm{POM2D}} - \mathbf{v}_{\mathrm{i,j-1,k}}^{\mathrm{POM2D}}}{2\Delta Y} \right\} \right)\,.$$

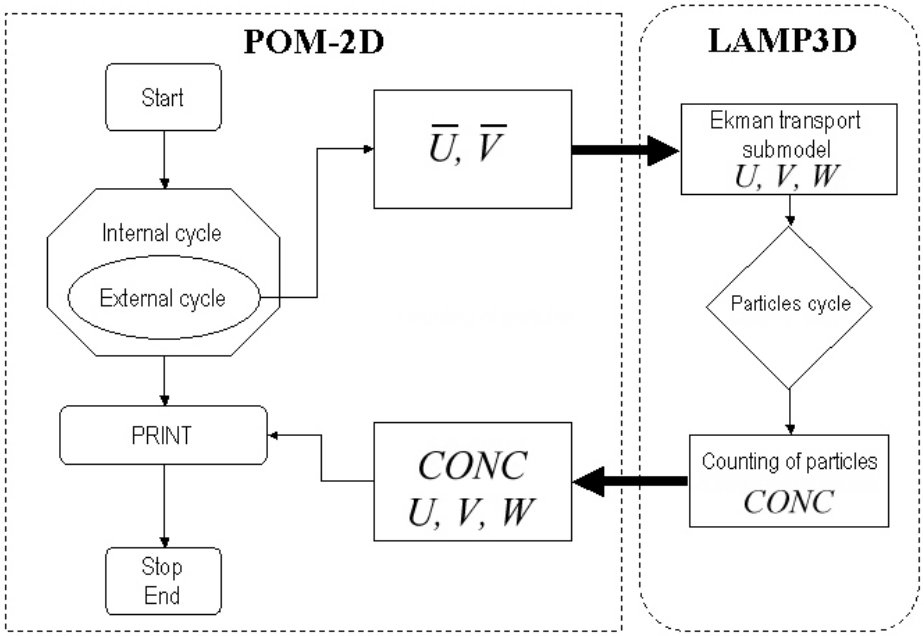

Fig. 2. Coupled model flow chart ($\overline{U}$=depth averaged along-shore component of velocity, $\overline{V}$=depth averaged cross-shore component of velocity, U=along-shore component of velocity, V=cross-shore component of velocity, W=vertical component of velocity, $CONC$=number of particles per mesh grid).

The deterministic velocity of each diffusing particle is determined through a weighted interpolation of velocity at the eight nearest neighbouring grid points.

The interactions between the hydrodynamic model POM2D and the dispersion (i.e. advection-diffusion) LAMP3D model is shown in Fig. 2.

2.4 Model setup and assumptions

2.4.1 Hydrodynamic characteristics

Astraldi and Manzella (1983) provided a complete analysis of hydrodynamic features in the study area, based on flow and temperature data offshore Lavagna. Data shows a nearly permanent flow of whole water mass towards North-West, parallel to the coast, with only short inversion time periods. This flow appears coherent at all depths, and the superficial (16-m depth) along-shelf component of velocity is close to 0.25 m/s for long periods. Maximum surface current recorded is close to 1 m/s, in association with very strong winter winds. Near the bottom (96-m depth) the velocity falls close to 0.1 m/s with a maximum of 0.4 m/s. The general circulation of the zone is connected to an along-shelf current due to density gradients and to the variations of the free

surface induced by wind (Esposito and Manzella, 1982).

2.4.2 Bathymetry

Bathymetry is essential to generate near-bottom forcings that need to be included in the hydrodynamic model. Bathymetric data were obtained by matching two digital charts of the Hydrographic Institute of the Italian Navy. The horizontal resolution is 400 m (along-shelf direction) $\times$ 200 m (cross-shelf direction). The original charts were lacking for depth $>$ 200 m, thus grid values were assigned by a linear interpolation up to the depth of 310 m due south. At the eastern and western boundaries two additional areas 15 meshes large have been artificially added in order to avoid numerical instabilities. To obtain the main flow direction perpendicular to the open boundaries of the numerical domain, the whole grid has been rotated by 12 degrees anticlockwise with respect to true North, using *ad hoc* programs.

2.4.3 Open boundaries conditions

Our domain has three open boundaries (northern boundary is 'closed' by the coast). A 'zero elevation' condition is assigned on southern boundary together with a 'zero gradient' condition for tangential and normal velocity. On eastern and western boundaries a 'zero gradient' condition for the velocity is assumed. In order to allow gravity wave outflow, a 'gravity radiation' condition is applied to elevation on eastern and western boundaries:

$$\frac{\partial \eta}{\partial t} \pm \sqrt{gH}\, \frac{\partial \eta}{\partial x} = 0 \, ,$$

where η is the sea surface elevation. To test the setup for open boundary conditions, some calibration runs with simplified bathymetry were performed, providing results coherent with those of other numerical experiments (Chapman, 1985).

2.4.4 Forcings evalutation

Coherently with the analysis by Astraldi and Manzella (1983), our hydrodynamic model was forced by the wind. Thus, the wind-setup induced elevation was also taken into consideration. The work of Ravasco (2000) provides a fair statistical treatment of wind data taken by the Italian Air Force since 1963 to 1996 at the Genoa airport *Cristoforo Colombo*. It was important to identify typical local winds both statistically and in their time evaluation, in order to simulate the typical wind-induced currents of the area. The analysis clearly shows the presence of three wind trends in the sectors of North-East (NE),

Time *(days)*	Wind direction *(degrees)*	Wind intensity *(m/s)*
$t_0 < t \leq 6$	$50^o NE$	7
$6 < t \leq 6.5$	$Calm$	–
$6.5 < t \leq 9.5$	$150^o SE$	3
$9.5 < t \leq 10$	$Calm$	–
$10 < t \leq 12$	$210^o SSW$	10

Table 1
Direction, intensity and blowing time used for wind in the 12 days simulation.

South-East (SE) and South-South-West (SSW). The NE wind channel is more frequent than the other two channels during the whole year, but mainly in winter. On the other side SE and SSW channels are more frequent during summer. The central directions of these three channels are $50^o, 150^o, 210^o$ for NE, SE, SSW respectively, with different spreading ranges.

Several previous simulations starting from a 'rest' condition (zero elevation, zero velocity and zero surface wind) and forced by the three different kinds of wind were used to verify the accuracy of the model with real bathymetry. The test simulation with NE wind of 7 m/s constant for 10 days provided information on coastal circulation corresponding to the most frequent wind regime. Finally, a complete twelve-day hydrodynamic simulation was carried out, starting from a 'rest' initial condition with wind direction and speed changing during the simulation in conformity with a typical local sequence (Corazza, ARPAL-CMIRL, Meteo-Hydrological Center of Liguria Region, pers. comm.; Table 1). Observed wind at 10 m above sea level, $\boldsymbol{v}_{10} = (u_{10}, v_{10})$, was used to determine the superficial boundary condition for the hydrodynamic model by the formulae:

$$\boldsymbol{\tau}^{\text{Wind}} = \frac{\rho_{\text{air}}}{\rho_{\text{water}}} C_{\text{d}} \boldsymbol{v}_{10} \sqrt{u_{10}^2 + v_{10}^2}\,,$$

where C_{d} is a suitable non-dimensional drag coefficient of order of magnitude 10^{-3} (Mattioli, 1993).

Input parameters used in the coupled model are summarized in Table 2.

2.4.5 Waste indicators

Dry pellet (ECOMAR, VERONESI VERONA s.p.a.) used in the marine fish farm consists of proteins (44.5% of weight), carbohydrates (15%) and lipids (23%). The remaining fraction is made up of ash (10%), phosphorus (1.35%)

Physical domain (km)	46x16
Horizontal resolution (m)	400x200
Vertical resolution (m)	10
Barotropic cycle time step (s)	1
Smagorinsky diffusivity coefficient	0.1
Asselin filter coefficient	0.05
Ekman depth δ_E (m)	150
Wind drag coefficient C_d	0.001
Horizontal standard deviation σ (m)	3.46
Particle cycle time step (s)	60
Number of particles	86400

Table 2
Input parameters used in the POM-LAMP3D coupled model simulations runs.

and fibre (1%). Nitrogen, phosphorus and organic carbon in uneaten feed, faecal matter and in excretion products were assessed in simulations. Excretion products consisted mainly of ammonia-bound nitrogen released through the gills and of phosphorus excreted as ortho-phosphate via the urine. Nitrogen and phosphorus are thus present in both soluble and, together with organic carbon, particulate form. For nitrogen and phosphorus it was necessary to define the soluble and particulate fractions, as well.

Nitrogen and phosphorus in faecal matter and excretion products

The nitrogen and phosphorus loads from a sea-cage depend on the food conversion ratio and on the nitrogen and phosphorus content in the feed used, therefore the nutrient load can vary greatly among different cages. The nutrient load from a cage is the difference between what is supplied with the feed and what is utilized by the fish for their growth as it is shown in Eq. (3) (Ackefors and Enell, 1990; Wallin and Håkanson, 1991):

$$\begin{aligned} n_{\text{rel}} &= n_{\text{supplied}} - n_{\text{used}} = \\ &= P * F_c * Cdn - P * Cfn = P * (F_c * Cdn - Cfn) \end{aligned} \tag{3}$$

where:
n_{rel} = nutrient load released (kg/year),
P = fish production (kg wet weight/year),
F_c = food conversion ratio (kg pellet used/kg fish produced),
Cdn = nutrient concentration in feed (% wet weight),
Cfn = nutrient concentration in fish (% wet weight).

In our case $P = 200000$ kg/year and $F_c = 1.3$ kg pellet used/kg fish produced.

Usually, nitrogen concentration in feed (CdN) varies from 6% to 7.3% whereas phosphorus (CdP) varies from 1.1% to 1.5% (Wallin and Håkanson, 1991; National Pollutant Inventory, 2001; Lupatsch and Kissil, 1998). Values used in the simulations are $CdN = 6.6\%$ and, provided by the feed producer, $CdP = 1.35\%$.

Many experimental works report nutrient concentration in fish. According to Wallin and Håkanson (1991), nitrogen and phosphorus content in rainbow trout (*Oncorhynchus mykiss*) are on average $CfN = 2.66\%$ and $CfP = 0.48\%$. The same values were found by Enell (1995) $CfN \simeq 3\%$ and by Lall (1991) $CfP = 0.4\% - 0.5\%$. According to Lupatsch and Kissil (1998), average phosphorus concentration in a gilthead seabream culture is $CfP = 0.72\%$, because it seems that phosphorus retention in *Sparus aurata* is greater than in other fish. Values used in the simulation are $CfN = 3\%$ and $CfP = 0.4\%$.

Ackefors and Enell (1990) found that 78% of nitrogen released is dissolved while the rest is particulated. For phosphorus, 21% is dissolved and 79% is particulate. Similar values were found by Lupatsch and Kissil (1998): dissolved nitrogen is 78%, particulate is 22%; dissolved phosphorus is 27% and particulate is 73%. This small discrepancy in phosphorus values may be due to the greater phosphorus retention in *Sparus aurata*.

Lupatsch and Kissil (1998) also investigated the subsequent solubility of faeces when falling under the sea cage. According to this research, of the total nitrogen released 13% is particulate, and the remainder is soluble and of the total phosphorus released 62% remains particulate. For our simulations the values of Ackefors and Enell (1990) are used.

The importance of the separation in dissolved and in particulate fractions for the simulations is due to the settling rate associated with the sedimentable fraction. Settling rate of faecal matter was studied by various authors. In the simple dispersion model of Gowen et al. (1989) fish faecal matter settling rate is 4 cm/s. From 50 observations Panchang et al. (1997) obtained a mean settling rate of 3.2 cm/s with 70% of the observation between 2 and 4 cm/s. Chen et al. (1999b) conducted laboratory experiments on the faecal pellets of caged Atlantic salmon and obtained significant differences in settling velocity as result of different salinity but not on the size of pellets. Mean settling velocity for pellets with mean length < 5 mm is 5.4 cm/s at 33 psu. Furthermore, in a recent paper Cromey et al. (2002a) used a mean settling velocity of faeces of 3.2 cm/s. Unfortunately, there is no data for Sea Bass and Sea Bream in the Mediterranean. Thus, considering the high salinity of the Mediterranean and the smaller size of reared fishes, we varied the settling velocity w_{sed} between 2 and 4 cm/s.

	Uneaten feed	Faecal pellet	Dissolved matter
N	2.35	0.93	3.32
P	0.48	0.81	0.22
C	16.00	0.04	

Table 3
Wastes indicators (g/particle) for numerical particles in the POM-LAMP3D coupled model simulation runs.

On the base of our assumptions the conversion factors of 3.32 g/particle and 0.22 g/particle were used for dissolved nitrogen and phosphorus respectively, and 0.93 g/particle and 0.81 g/particle for faecal nitrogen and phosphorus respectively.

Nitrogen and phosphorus in uneaten feed

The percentage of feed that goes uneaten and sinks as waste varies between 1% and 40%. Findlay and Watling (1994) recommend the use of a value of 5% or lower for modern aquaculture farms.

Settling rate of feed is different from that of faecal matter. Gowen et al. (1989) used a settling velocity equal to 12 cm/s. Findlay and Watling (1994) provided data on several North American pellet types or sizes and quote settling rates of 5.5 cm/s and 15.5 cm/s for 3 mm and 10 mm dry pellets, respectively. Elberizon and Kelly (1998) showed settling velocities of freshwater salmonid pellet diets ranging from 5 to 12 cm/s for 2 mm and 8 mm pellet sizes, respectively. This results are similar to settling rates found by Chen et al. (1999a), who studied the physical characteristics of commercial pelleted Atlantic salmon feeds finding that the temperature and the salinity of sea water significantly influence the settling velocity. Again literature data are lacking regarding Sea Bream and Sea Bass in the Mediterranean. In our case the feed size varies between 4-4.5 mm (ECOMAR 4) and 6.8-7.7 mm (ECOMAR 7). The near-surface temperature measurements by Astraldi and Manzella (1983) show a seasonal trend with mean values decreasing from 22^{o}C in the summer season to 14^{o}C in the winter season. Same authors reported that no significant differences in salinity could be found over the area, except for local intrusion of fresh water. Taking as mean salinity the value of 37 psu, we varied the settling velocity w_{sed} between 6 and 12 cm/s.

On the base of our assumptions the conversion factors of 2.35 g/particle and 0.48 g/particle were used for nitrogen and phosphorus released from uneaten feed respectively.

Organic carbon in faecal matter and in uneaten feed

The organic carbon fraction in feed and faecal matter can vary greatly. Findlay

and Watling (1994) proposed the value of 45% and 28% for feed and faecal matter, respectively. Dudley et al. (2000) used for modeling the value of 1.9 g of faeces produced for kg of fish. Thus, in our case (200 ton/year of fish) we should have about 380 kg/year of faeces produced.

On the base of our assumptions the conversion factors of 0.04 gC/particle and 16 gC/particle were used for faecal and uneaten feed respectively.

The assumption and the weigths given to numerical particles for waste indicators are summarized in Table 3.

Information available in literature on decomposition rates of faecal material and uneaten feed is scarse. Avnimelech et al. (1995) evaluated the first order kinetic rate constants for organic carbon and organic nitrogen degradation. More recently, van Rijn and Nussinovitch (1997) proposed an empirical model of degradation of organic solids. Since the smallest estimate found for T_{90} ($\simeq$ 2 months) is in any case greater than time period simulated, we considered the particles to be conservative. Moreover, in literature we did not find estimates of the removal of waste food and faecal pellets arising from the farmed fish by wild fish. Therefore, we assumed that the likelihood for a pellet (feed and faeces) to reach the bottom is 100%.

3 Results and discussion

3.1 Water circulation

With NE and SE wind the current follows the coast moving westward until it reaches the cape where flow separation occurs with consequent generation of a leeward eddy (Fig. 3ab). In contrast, with SSW wind the nearshore current intensifies as consequence of water accumulation toward the coast and there is the generation of an upstream eddy (Fig. 3c).

The modeled wind-driven circulation shows clearly the presence of the westward transport observed by Astraldi and Manzella (1983). Qualitative comparison with other numerical experiments also agrees (Baldi et al., 1997).

Under the cages the current intensity decreases almost linearly with depth (Fig. 4). There is a difference in the rate of decrease in speed according to wind intensity and direction. SSW wind produces the highest superficial current.

(a)

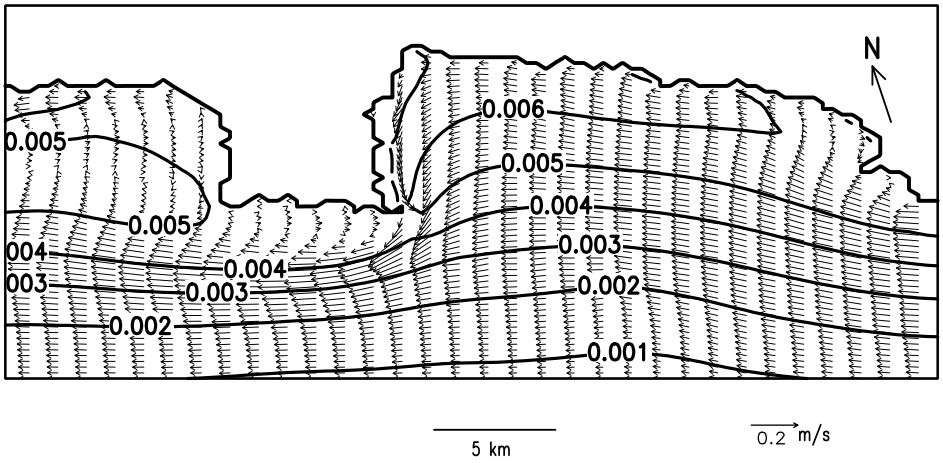

(b)

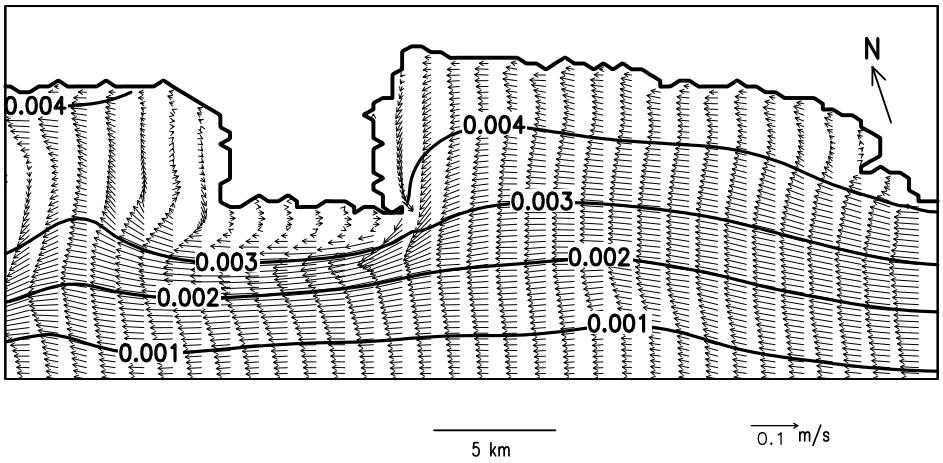

(c)

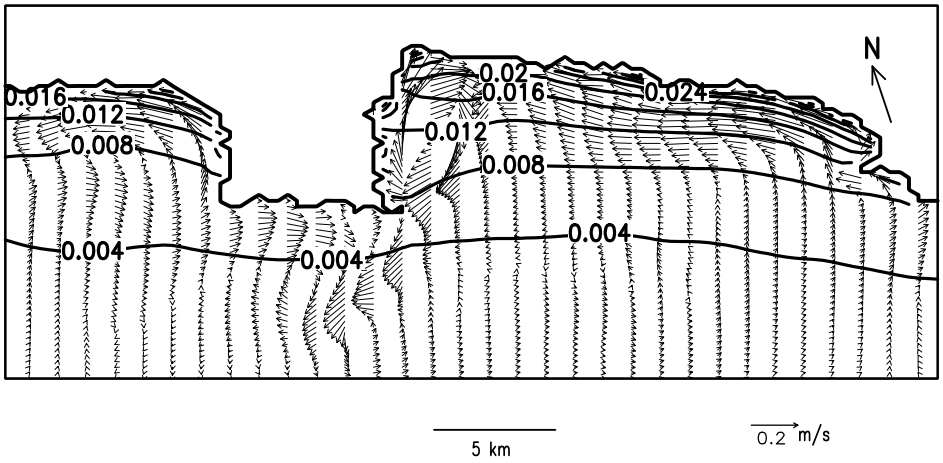

Fig. 3. Depth averaged velocity (arrows [m/s]) and elevation (contour lines [m]) fields calculated for (a) *NE* wind (b) *SE* wind and (c) *SSW* wind.

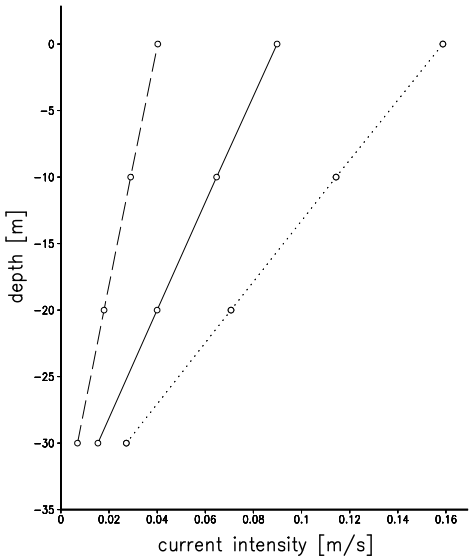

Fig. 4. Current intensity profiles under the cages for the NE wind (solid line), SE wind (dashed line) and SSW wind (dotted line).

3.2 Dispersion and settling of aquaculture wastes

Three simulation scenarios were used to estimate the fate of pollutants:

- a continuous release of particles without settling rate for assessesing the impact of dissolved nutrients;
- a continuous release of particles with a settling rate of $0.02 - 0.04$ m/s for assessing the impact of faecal matter;
- releasing once a day of particles with a settling rate of $0.06 - 0.12$ m/s for assessing the impact of wasted feed.

Though it is presently well known that fish farm effect on the environment is mainly confined to the sediment compartment (via settling of coarse particles) (Karakassis et al., 2000), we included dissolved nutrient simulation for completeness sake, as this is a first study, and for testing the overall numerical study method.

3.2.1 Simulations for dissolved nutrients

Nutrients are first carried by the along-shelf current generated by the NE wind and follow the coast until they arrive at the headland of Portofino (Fig. 5a). In Portofino they spread towards the open sea due to strong currents. They cannot spread west due to the boundary between currents and leeward eddy. With the onset of SE wind the water flows slowly for the duration of the wind and leads to a concentration of nutrients toward the coast (Fig. 5b). The scenario rapidly changes whit the SSW wind (Fig. 5c). Concentrated nutrients

(a)

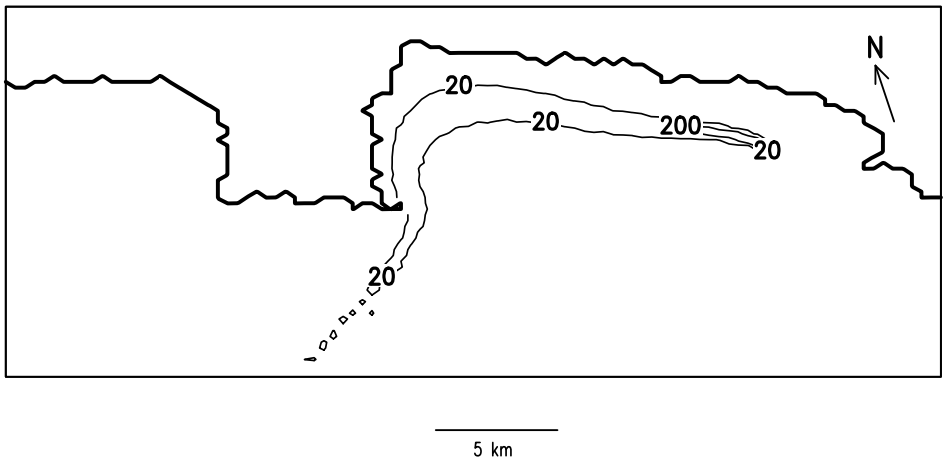

(b)

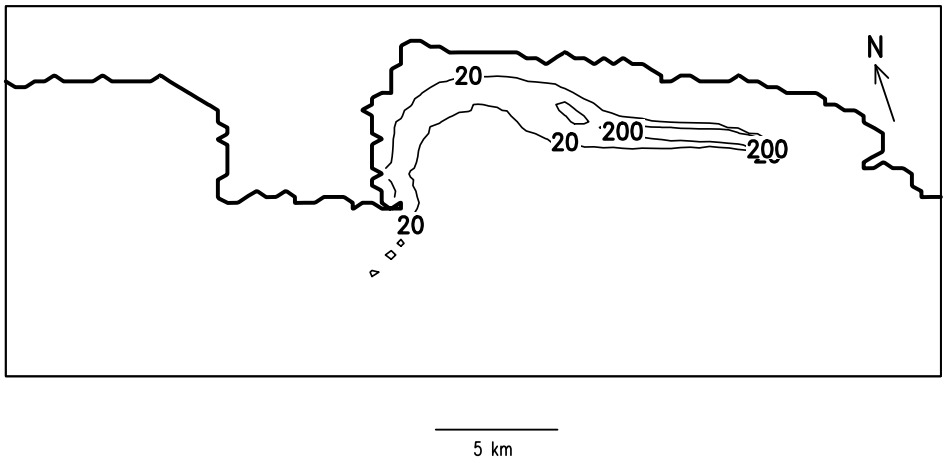

(c)

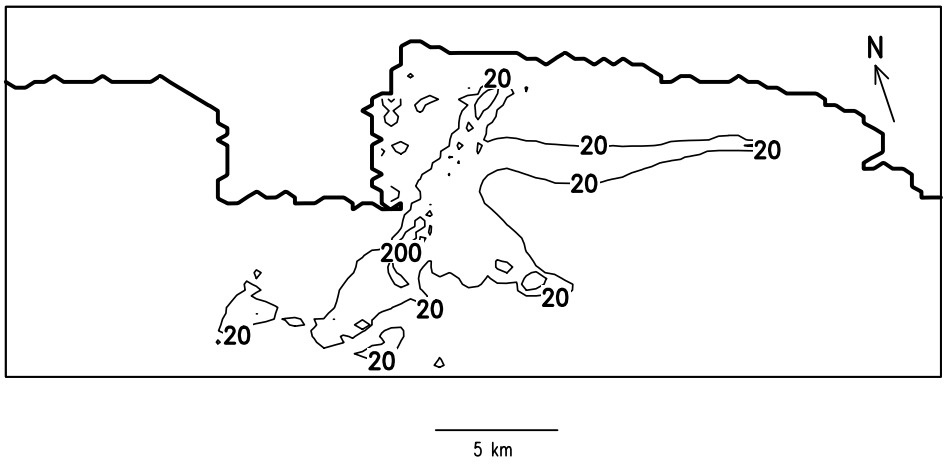

Fig. 5. Dispersion for dissolved matter calculated by the model for (a) NE wind (b) SE wind and (c) SSW wind. The results are expressed as number of particles per mesh grid: 200 particles correspond to 0.83 μgN/l and 0.06 μgP/l.

(a)

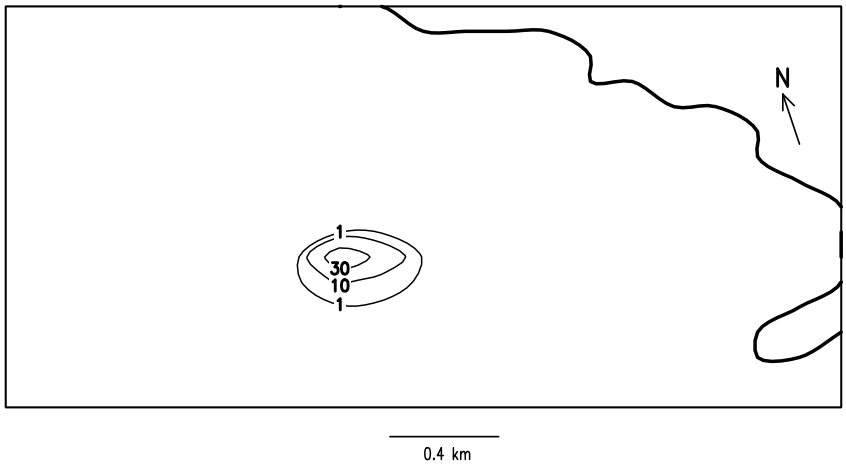

(b)

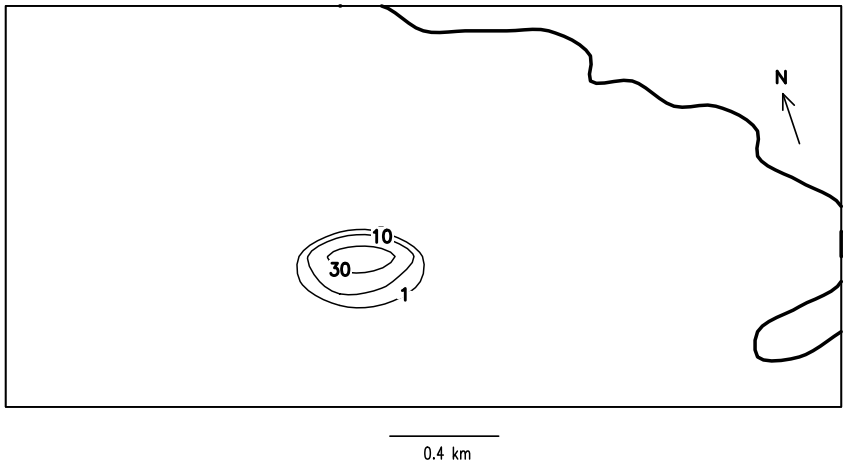

Fig. 6. Dispersion for particulated matter calculated by the model at the end of the simulation (12 days). (a) Faecal pellets with w_{sed}=0.04 m/s, 10 particles correspond to 0.12 gN/m^2, 0.10 gP/m^2 and 0.005 gC/m^2. (b) Uneaten feed with w_{sed}=0.12 m/s, 10 particles correspond to 0.03 gN/m^2, 0.006 gP/m^2 and 0.2 gC/m^2.

remain trapped in a big eddy with a clear accumulation in the center of the Golfo del Tigullio. In all simulations, the highest concentrations calculated by the model rarely exceed 4 μg/l of total dissolved nitrogen and 1 μg/l of total dissolved phosphorus.

3.2.2 Simulations for particulate matter

The dispersion of particulate matter was not sensitive to release schedules or settling rates. Particulate matter, therefore, remained in the vicinity of net-pens (Fig. 6). The imposed settling velocity, comparable with the local current velocity, carries uneaten feed to the sea bottom more rapidly than

	Faeces	Feed
Nitrogen	0.049	0.012
Phosporus	0.042	0.003
Organic carbon	0.002	0.083

Table 4
Highest loading rates for faecal and feed matter calculated by the model (express as $g/m^2/day$).

faecal pellets because dispersion of faecal pellets is more strongly influenced by dominating current.

To carefully assess the fate of the particle once on the bed we have to consider resuspension processes. The magnitude of the current after wich resuspension becomes critical is debatable. For fish farm wastes, Dudley et al. (2000) conducted a fieldwork to improve parametrization of erodibility in the transport model of the AWATS package and reported a high critical thresold of resuspension between 0.33 and 0.66 m/s. Conversely, Cromey et al. (2002b) obtained best fit with a low critical resuspension speed of 0.095 m/s for DEPOMOD resuspension model. Recently in the Mediterranean, Palanques et al. (2002) measured near-bottom currents and water turbidity in combination with wave data on the microtidal Ebro continental shelf. At 12-m depth resuspension by waves occurs during one third of the time, whereas resuspension by currents only occurs sporadically. At 60-m depth waves can only resuspend the cohesive mud, in association with the strongest storms. Resuspension by currents does not occur. Their conclusion is that Mediterranean shelf differs from locations characterized by strong tides and long period waves. Our model calculates a 30-m depth velocity lower than 0.04 m/s for all the simulations (Fig. 4). This value is less than the lower critical thresolds proposed for fish farm wastes (Cromey et al., 2002b). At the end of our simulations particle number never exceeds 50000 and 5000 particles/grid mesh for faecal and feed matter respectively (Table 4).

To assess the environmental impact of fish cages we need to determine if the organic enrichment could exceed the assimilation capacity of the environment. The estimated theoretical maximum aerobic oxidation for an environment with a minimum two-hour average current velocity of 4 cm/s is nearly 17 g $C/m^2/day$ (Findlay and Watling, 1994). Following Cromey et al. (1998) who used the values provided by Marine Ecosystem Research Laboratory, organic loading rates less than 36 $gC/m^2/year$ have little effect, rates between 36-365 $gC/m^2/year$ enrich the sediment community and a loading over 548 $gC/m/m^2/year$ produced degraded conditions. The maximum average loading rate calculated for organic carbon by our model is 0.085 $gC/m^2/day$, which corresponds closely to 36 $gC/m^2/year$, assuming no seasonal variation.

	Observations [m/s]					Model Output [m/s]			
	Winter average (std)	Spring average (std)	Summer average (std)	Autumn average (std)	Annual average (std)	NE wind day 6	SE wind day 9	SSW wind day 12	12 days average
C1	0.066 (0.057)	0.075 (0.065)	0.063 (0.052)	0.070 (0.052)	0.069 (0.057)	0.072	0.028	0.081	0.062
C2	- -	- -	0.080 (0.052)	- -	- -	0.096	0.036	0.088	0.074

Table 5
Comparison between current measurements and model outputs at 20-m depth.

In conclusion concentrations of elemental wastes predicted by the model are low in the investigated area in both water column and sediment compartments and never exceeded the threshold for environmental concern.

3.3 Comparison with pre-existing field data

3.3.1 Currents

Current data simulated by the model were compared with data provided by the National Research Council (CNR) and the Italian National Agency for New Technologies, Energy and Environment (ENEA) from the SIAM database. These data were collected by two current meters, C1 and C2, located at 2 km and 3 km distance west of the farm, respectively. Current speed and direction were sampled every hour at 20 m depth from February 1993 to March 1994 (C1) and from August to October 1997 (C2).

The overall seasonal averages of intensity calculated from C1 data are very close to the value obtained forcing the model with the NE wind, which is the most frequent wind (Table 5). Similarly, SE and SWW data from the model are always within the range of seasonal average $\pm$ std value from C1 measurements. The 12 days average modeled current is in good agreement both with winter and summer averages as well as the annual average (Table 5). The greater intensity observed in the C2 station is found in the modeled data and it is within the range of field observations. Ultimately, current direction as calculated by the model agrees with the observed northwestward along-shore water movement. Some period of southeastward current movement was also observed at the end of the 12 days simulation with SSW wind.

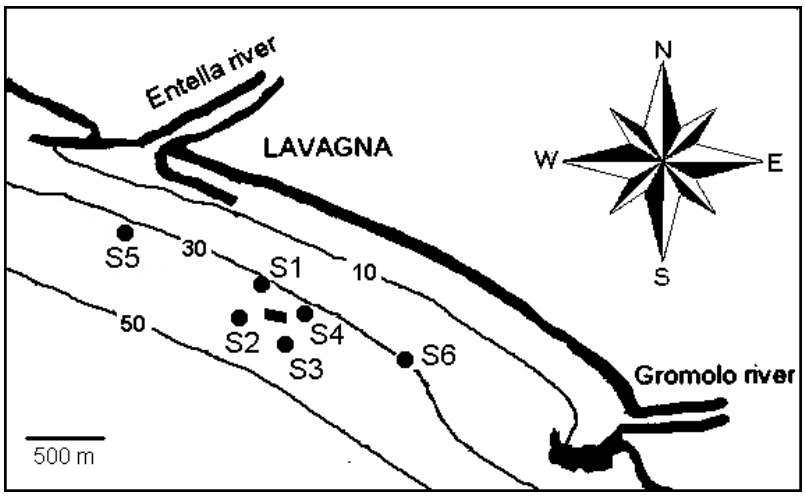

Fig. 7. Location of the sampling stations (circles) for collection of experimental data near the net-pen system (square).

3.3.2 Nutrients

First available data in the area were collected periodically from July 2000 to August 2002 as requested from farmers by local public authority. Water and sediment samples were collected in 6 stations in the area surrounding the fish farm (Fig. 7). Water was sampled nine times at surface and bottom with a Niskin bottle and analyzed spectophotometrically for nitrate (detection limit = 0.7 μmol/l) and phosphate (detection limit = 0.2 μmol/l). Sediment was sampled three times using a Van Veen grab and analyzed for total nitrogen and total phosphorus.

In most of the stations, concentrations of nutrients in the water column was below instrument detection limits. This agrees with modeled data that provides very low concentrations for dissolved nitrate (less than 0.083 μgN/l) and phospate (less than 0.06 μgP/l). Occasionally, higher nutrient concentrations recorded in field data (up to 15.1 μmol/l and 1.8 μmol/l in station S6 for total nitrogen and phosphorus, respectively) were due to the nutrients discharge from the Entella and Gromolo rivers, following rainfall. Because our model was not developed to detect potential impacts from sources other than fish cages, we did not detect nutrient due to rainfalls. The very low concentration of nutrients found in bottom samples confirm the resuspension to be negligible.

Field sediment nutrients data were highest in station S2 and lowest in station S4, wich agrees with model observations for total nitrogen and phosphorus under westward transport. Daily loading rate between field and modeled data were also in agreement (Fig. 8). More difficult is the comparison of absolute values. In fact, to express in the same units the modeled and experimental data we need heavy assumptions on the sediment density as well as on the sampling methodology. Furthermore, accurate estimates of historical data are difficult

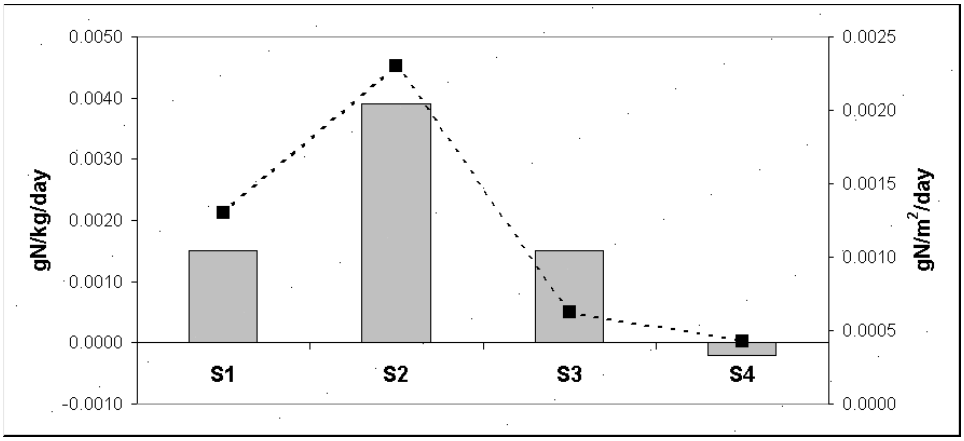

Fig. 8. Daily nitrogen loading rate observed (bar, [g/kg/day]) and modeled (dotted line, [g/m^2/day]).

to obtain. For assignment of weigths to numerical particles we need detailed information on the reared biomass and food supply that are not available.

Future developments will need to validate the model on a regional scale with field sampling and monitoring. Collaboration with farmers is essential for data collection. Thereafter, key biological processes such as biodegradation and the role of wild fish may be included in a model such as ours.

4 Conclusions

Aquaculture dispersion models aim to provide quantitative estimates of the possible environmental consequences of fish farming, thus offering a useful tool for regulatory and mitigation purposes (Silvert and Sowles, 1996). Although a number of aquaculture models has been developed for cold water areas (Gowen et al., 1989; Ross et al., 1993a, 1994, 1993b; Gillibrand and Turrell, 1997; Panchang et al., 1997; Dudley et al., 2000; Cromey et al., 2002a), models for Mediterranean Sea are generally lacking. The predictions of pollutant dispersion and deposition in density/wind driven Mediterranean systems is one of the key question currently asked for modeling the environmental effects of fish cage farming. We linked the Langragian particle model LAMP3D to the more complex hydrodynamic model POM, which has the potential for providing predictions for the length of a wind record. The aim of this model is to serve the mariculture industry in avoiding environmental impacts of their operations by providing a tool for assessing farm management scenarios. This is expected to aid decision making on topics such as: appropriate sites for fish farm establishment; optimization of reared biomass and production targets; realistic forecasting for the development of a larger aquacultural industries. In this way data requirements may be met by farmers undertaking monitoring

programs. Further extending our study to other locations where fish cages operate in the Mediterranean Sea may contribute to an improvement in the field of management and decision making of net-pen aquaculture.

Acknowledgements

We wish to thank Annalisa Griffa for her precious help with mathematical modelling and Roberto Festa for his useful advices. We would like to acknowledge the support provided by INFM - National Institute for the Physics of Matter and in particular to Corrado Ratto. More thanks to Mauro Fabiano for his assistance in the interpretation of environmental data. We also thank the Regione Liguria for support and collaboration. We thank Antonio Schirone for precious help with the current data, gently provided by the National Research Council (CNR) and the Italian National Agency for New Technologies, Energy and Environment (ENEA) from the SIAM database and Maurizio Costa for the environmental data. We are grateful to Giorgio Fanciulli and the staff of AQUA s.a.s. for their collaboration. We finally thank the anonymous reviewers for the constructive criticism and support to the original manuscript.

References

Ackefors, H., Enell, M., 1990. Discharge nutrients from swedish fish farming into adjacent sea areas. Ambio 19 (1), 28–35.

Allen, C., 1982. Numerical simulation of contaminant dispersion in estuarine flow. Proc. R. Soc. Lond. A 381, 179–194.

Astraldi, M., Manzella, G., 1983. Some observations on current measurements on the East Ligurian Shelf, Mediterranean Sea. Continental Shelf Research 2, 183–193.

Avnimelech, Y., Mozes, N., Diab, S., Kochba, M., 1995. Rates of organic carbon and nitrogen degradation in intensive fish ponds. Aquaculture 134, 211–216.

Bacciola, D., Borghini, M., Degl'Innocenti, F., Galli, C., Lazzoni, E., Meloni, R., Sparnocchia, S., Cannarsa, S., Di Fesca, V., Manzella, G. M. R., Marri, P., Raso, G., 1993. Esperimenti per la determinazione del coefficiente di diffusione locale. Tech. rep., ENEA, RTI/AMB/GEM-MAR/93/07.

Baldi, P., Marri, A., Schirone, A., 1997. Applicazione di un modello per la simulazione del trasporto e della diluizione di inquinanti nelle acque costiere. Tech. rep., ENEA, RTI/AMB/GEM-MAR/97/04/RL2/A1.4.

Chapman, D., 1985. Numerical treatment of cross-shelf open boundaries in a barotropic coastal ocean model. Journal of Physical Oceanography 15 (8), 1060–1075.

Chelossi, E., Vezzulli, L., Milano, A., Branzoni, M., Fabiano, M., Riccardi, G., Banat, I., 2003. Antibiotic resistance of benthic bacteria in fish-farm and control sediments of the Western Mediterranean. Aquaculture 219 (1-4), 83–97.

Chen, Y., Beveridge, M., Telfer, T., 1999a. Physical characteristics of commercial pelleted atlantic salmon feeds and consideration of implications for modeling of waste dispersion through sedimentation. Acquaculture International 7, 89–100.

Chen, Y., Beveridge, M., Telfer, T., 1999b. Settling rate characteristics and nutrient content of the faeces of Atlantic salmon, *Salmo salar* L., and the implications for modelling of solid waste dispersion. Acquaculture Research 30, 395–398.

Cromey, C., Black, K., Edwards, A., Jack, I., 1998. Modelling the deposition and biological effects of organic carbon from marine sewage discharges. Estuarine, Coastal and Shelf Sciences 47, 295–308.

Cromey, C., Nickell, T., Black, K., 2002a. DEPOMOD-modelling the deposition and the biological effects of wastes solids from marine cage farms. Aquaculture 214 (1-4), 211–239.

Cromey, C., Nickell, T., Black, K., Provost, P., Griffiths, C., 2002b. Validation of a fish farm waste resuspension model by use of a particulate tracer discharged from a point source in a coastal environment. Estuaries 25 (5), 916–929.

Doglioli, A., 2000. LAMP3D, un modello Lagrangiano per lo studio della dispersione di inquinanti in acque costiere. Master Thesis, Università degli Studi di Genova.

Dudley, R., Panchang, V., Newell, C., 2000. Application of a comprehensive modeling strategy for the management of net-pen aquaculture waste transport. Aquaculture 187, 319–349.

Elberizon, I., Kelly, L., 1998. Settling measurements of parameters critical to modelling benthic impacts of freshwater salmonid cage aquaculture. Acquaculture Research 29, 669–677.

Enell, M., 1995. Environmental impacts of nutrient from nordic fish farming. Water Science Technologies 31 (10), 61–71.

Esposito, A., Manzella, G., 1982. Current circulation in the Ligurian Sea. In: Nihoul, J. (Ed.), Hydrodynamics of semi-enclosed seas. Elsevier Scientific Publishing Company, Amsterdam, pp. 187–204.

Findlay, R., Watling, L., 1994. Toward a process level model to predict the effects of salmon net-pen aquaculture on the benthos. In: Hargrave, B. (Ed.), Modeling Benthic Impacts of Organic Enrichment from Marine Aquaculture. Canadian Technical Report of Fisheries and Aquatic Sciences 1949: xi + 125 p.

Gillibrand, P., Turrell, W., 1997. The use of simple models in the regulation of the impact of fish farms on water quality in Scottish sea lochs. Aquaculture 159, 33–46.

Gowen, R., Bradbury, N., Brown, J., 1989. The use of simple models in assess-

ing two of the interactions between fish farming and marine environment. In: DePauw, N., Jaspers, E., Ackefors, H., Wilkins, N. (Eds.), Aquaculture - A Biotechnology in Progress. European Aquaculture Society, pp. 1071–1080.

Henderson, A., Gamito, S., Karakassis, I., Pederson, P., Smaal, A., 2001. Use of hydrodynamic and benthic models for managing environmental impacts of marine aquaculture. Journal of Applied Ichthyology 17, 163–172.

Karakassis, I., Tsapakis, M., Hatziyanni, E. Papadopoulou, K., Plaiti, W., 2000. Impact of cage farming of fish on the seabed in three Mediterranean coastal areas. ICES Journal of Marine Science 57 (5), 1462–1471.

Lall, S., 1991. Digestibility, metabolism and excretion in dietary phosphorus in fish. In: Cowey, C., Cho, C. (Eds.), Nutritional Strategies and Aquaculture Waste. University of Guelph, Guelph, Ontaria, pp. 21–36.

Lupatsch, I., Kissil, G., 1998. Predicting aquaculture waste from gilthhead seabream (*Sparus aurata*) culture using a nutritional approach. Aquatic Living Resources 11 (4), 265–268.

Magaldi, M., 2002. Applicazione del Princeton Ocean Model e del Lagrangian Assessment for Marine Pollution model per uno studio dell'impatto derivante da impianti di maricoltura. Master Thesis, Università degli Studi di Genova.

Mattioli, F., 1993. Principi Fisici di Oceanografia e Meteorologia. Editrice Compositori Srl, Bologna.

Mellor, G., 1998. Users Guide for a three-dimensional, primitive equation, numerical ocean model. Princeton University, Princeton, NJ 08544-0710.

National Pollutant Inventory, 2001. Emission estimation technique manual for aggregated emissions from temperate water finfish aquaculture. Commonwealth of Australia.

Palanques, A., Puig, P., Guillen, J., Jimenez, J., Gracia, V., Sànchez-Arcilla, A., Madsen, O., 2002. Near-bottom suspended sediment fluxes on the microtidal low-energy Ebro continental shelf (NW Mediterranean). Continental Shelf Research 22, 285–303.

Panchang, V., Cheng, G., Newell, C., 1997. Modeling hydrodynamics and aquaculture waste transport in Coastal Maine. Estuaries 20, 14–41.

Ravasco, I., 2000. Un modello stocastico misto per le serie temporali triorarie di ventosità a Genova. Master thesis, Università degli Studi di Genova.

Ross, A., Gurney, W., Heath, M., 1994. A comparative study of the ecosystem dynamics of four fjords. Limnology and Oceanography 39, 318–343.

Ross, A., Gurney, W., Heath, M., Hay, S., Henderson, E., 1993a. Astrategic simulation model of a fjord ecosystem. Limnology and Oceanography 38, 128–153.

Ross, L., Mendoza, Q., Beveridge, M., 1993b. The application of geographycal information systems to site selection for coastal aquaculture: an example based on salmonid cage culture. Aquaculture 112, 165–178.

Silvert, W., Sowles, J., 1996. Modelling environmental impacts of marine finfish aquaculture. Journal of Applied Ichthyology 12, 75–81.

Sørensen, B., Nielsen, N., Lanzky, P., Holten Lützhøft, H., Jorgensen, S., 1998.

Occurence, fate and effects of pharmaceutical substances in the environment - a review. Chemosfere 36 (2), 357–393.

Tsutsumi, H., Kikuchi, T., Tanaka, M., Higashi, T., Imasaka, K., Miyazaki, M., 1991. Benthic faunal succession in a cove organically polluted by fish farming. Marine Pollution Bulletin 23, 233–238.

van Rijn, J., Nussinovitch, 1997. An empirical model for predicting degradation of organic solis in fish culture systems based on short-term observations. Aquaculture 154, 173–179, Technical Note.

Vezzulli, L., Chelossi, E., Riccardi, G., Fabiano, M., 2002. Bacterial community structure and activity in fish farm sediment of the Ligurian Sea (Western Mediterrenean). Aquaculture International. 10 (2), 123–141.

Vezzulli, L., Marrale, D., Moreno, M., Fabiano, M., In press. Quantitative and qualitative changes of the meiofauna community in long-term impacted fish-farm sediments of the Ligurian Sea (Western Mediterrenean). Chemistry and Ecology .

Vismara, R., 1992. Ecologia Applicata 2^a edizione. Hoepli, Milano.

Wallin, M., Håkanson, L., 1991. Nutrient loading models for the assessment of environmental effects of marine fish farms. In: Marine Aquaculture and Environment. Nord 1991:22. Nordic Council of Ministers, pp. 39–55.

Wu, K., 1995. The environmental impact of marine fish culture: towards a sustainable future. Marine Pollution Bullettin 31, 159–156.

Wu, R., Lam, K., MacKay, D., Lau, T., Yam, V., 1994. Impact of marine fish farming on water quality and bottom sediment: a case study in the sub tropical environment. Marine Environmental Research 38, 115–145.

Zannetti, P., 1990. Air Pollution Modeling. Computational Mechanics Publications, Boston.

List of Figures

List of Tables

Contents